JACS
JOURNAL OF THE AMERICAN CHEMICAL SOCIETY
Article
pubs.acs.org/JACS

Activation of a Hydroamination Gold Catalyst by Oxidation of a Redox-Noninnocent Chlorostibine Z-Ligand

Haifeng Yang and François P. Gabbaï*

Department of Chemistry, Texas A&M University, College Station, Texas 77843-3255, United States

Supporting Information

ABSTRACT: In search of new platforms that support redox-controlled catalysis, we have investigated the noninnocent behavior of chlorostibine ligands coordinated to gold. The gold chlorostibine complex ((*o*-(Ph_2P)C_6H_4)$_2$SbCl)AuCl (**1**-Cl) undergoes a clean oxidation reaction on treatment with $PhICl_2$. This oxidation reaction affords the corresponding trichlorostiborane complex ((*o*-(Ph_2P)-C_6H_4)$_2$$SbCl_3$)AuCl (**2**-Cl), which can be converted into the more tractable trifluoride analogue ((*o*-(Ph_2P)C_6H_4)$_2$$SbF_3$)AuCl (**3**-Cl) by treatment with a fluoride source. As supported by experimental and computational results, these complexes possess a Au→Sb donor–acceptor interaction which is distinctly stronger in the oxidized complexes **2**-Cl and **3**-Cl. Both **1**-Cl and **3**-Cl undergo a clean chloride abstraction reaction to afford the corresponding cationic gold species [((*o*-(Ph_2P)C_6H_4)$_2$SbCl)Au]$^+$ ([**1**]$^+$) and [((*o*-(Ph_2P)C_6H_4)$_2$$SbF_3$)Au]$^+$ ([**3**]$^+$), which have been isolated as SbF_6^- salts. As a result of a stronger Au→Sb interaction, cation [**3**]$^+$ features a more Lewis acidic gold center. It forms an isolable water adduct and also activates terminal alkynes toward hydroamination with arylamines. These results demonstrate that the redox state of noninnocent Z-ligands can be used to control the catalytic activity of the adjoining metal center.

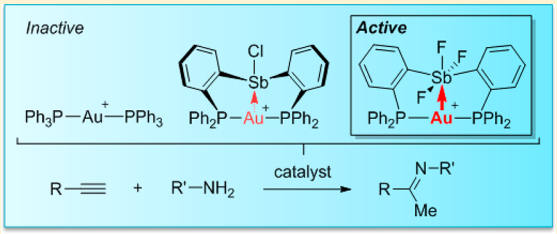

INTRODUCTION

While often regarded as heavy phosphine analogues, stibine ligands possess a number of unusual characteristics, including softer donor properties[1] combined with increased accepting properties.[2] We have also demonstrated that triarylstibine ligands are redox-noninnocent and can be converted from L-type (**A**) to Z-type ligands[3] (**B**) via oxidation (Chart 1).[4]

Chart 1. Oxidation of Coordinated Stibine Ligands

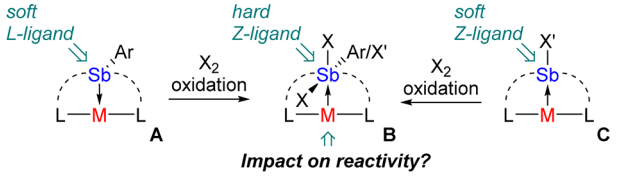

Oxidation proceeds without dissociation of the metal, provided that ancillary ligands are employed. This redox process has been shown to induce an umpolung of the M–Sb bond which switches from Sb→M in the reduced state to M→Sb in the oxidized state.[4a] Interestingly, σ-accepting properties are also observed with halostibine ligands (**C**).[5] In this case, oxidation of the antimony simply increases the Lewis acidity of the antimony center, making it a stronger σ-acceptor and thus a harder Z-ligand. While we have previously focused on the impact of oxidation on the nature of the metal–antimony bond, it occurred to us that such ligand-centered processes may provide control over the Lewis acidity and reactivity of the adjoining metal center.[6]

The hydroamination of alkynes is a powerful synthetic method which provides access to a diverse array of nitrogen-containing organic compounds. These hydroamination reactions are efficiently catalyzed by late-transition-metal complexes,[7] including gold complexes.[8] To date, most of the gold catalysts used are monoligated gold(I) complexes of the type [LAu]$^+$ in which the exposed and thus Lewis acidic metal ion is readily available for substrate activation. Two-coordinate gold(I) complexes of the type [L_2Au]$^+$ are not active, presumably because of the lack of Lewis acidity of the gold center. Inspired by a recent report describing the use of a gold–boron complex of the type [L_2Au→BAr_3]$^+$ as a catalyst for enyne cyclization,[9] we questioned whether the use of a redox-active Z-ligand such as a halostibine could afford a complex whose catalytic properties are controlled by the redox state of the Z-ligand (Chart 2). In this paper, we describe a chlorostibine gold complex whose catalytic activity for the hydroamination of alkynes is turned on by oxidation of the antimony center. These results add to the growing repertoire of redox-controlled catalytic processes[10] and illustrate the role that

Chart 2. Representation of Possible Catalyst Structures

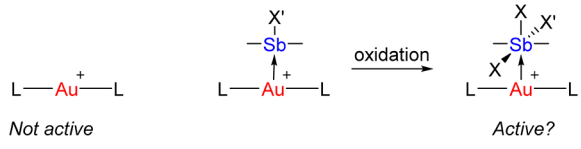

Received: July 30, 2015
Published: October 12, 2015

DOI: 10.1021/jacs.5b07998
J. Am. Chem. Soc. 2015, 137, 13425–13432

Z-ligands can play in the activation of otherwise inactive catalytic centers.[6,9,11]

RESULTS AND DISCUSSIONS

Gold-chlorostibine complexes. The chlorostibine–gold complex **1**-Cl was synthesized from the known ligand L^{Cl} [12] and Au(tht)Cl (Scheme 1). This complex, which is an analogue of

Scheme 1. Synthesis of 1-Cl and [1][SbF$_6$][13]

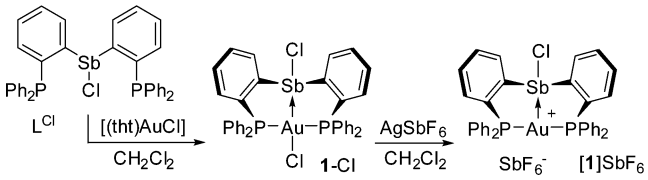

the known complex $[(o\text{-}(i\mathrm{Pr}_2\mathrm{P})\mathrm{C}_6\mathrm{H}_4)_2\mathrm{SbCl}]\mathrm{AuCl}$,[5] reacts with $AgSbF_6$ in dichloromethane to afford the air-stable salt [**1**][SbF_6]. The ^{31}P NMR spectrum of [**1**][SbF_6] features a signal at 50.3 ppm, significantly downfield from that of **1**-Cl at 38.4 ppm. Complexes **1**-Cl and [**1**][SbF_6] have been fully characterized, and their structures have been determined using single-crystal X-ray diffraction (Figure 1). In both complexes,

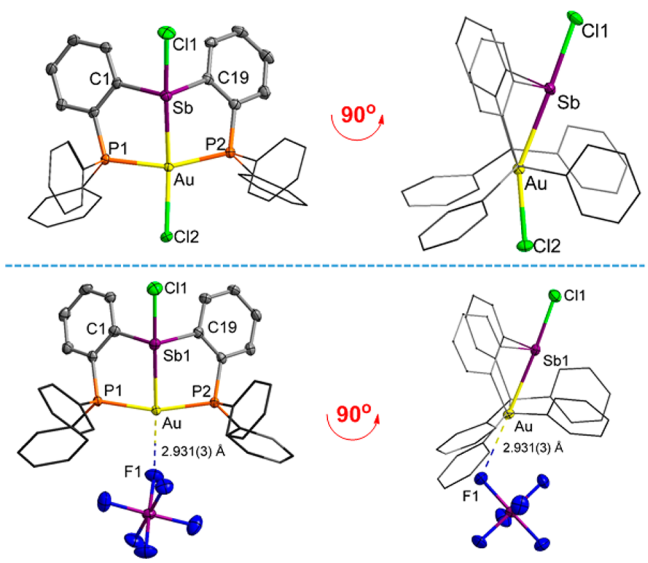

Figure 1. Solid-state structures of **1**-Cl (top) and [**1**][SbF_6] (bottom). Thermal ellipsoids are drawn at the 50% probability level. Phenyl groups are drawn in wireframe. Hydrogen atoms and solvent molecules are omitted for clarity. Relevant metrical parameters can be found in the text or the Supporting Information.

the antimony atom adopts a distorted seesaw geometry with a Cl(1)–Sb–Au angle close to linearity (177.00(3)° for **1**, 177.16(3)° for [**1**]SbF_6) and a compressed C(1)–Sb–C(19) angle (99.89(15)° for **1**-Cl, 98.08(13)° for [**1**][SbF_6]). The gold center of **1**-Cl displays a distorted square-planar geometry, with the chloride bending away from the Sb–Au vector by 26.10(3)°. The primary ligands of [**1**][SbF_6] are arranged about the gold atom in a distorted T-shaped geometry with P(1)–Au–Sb(1), P(2)–Au–Sb(1), and P(1)–Au–P(2) angles of 83.00(2), 81.39(3), and 159.46(4)°, respectively. The coordination sphere of the gold atom is completed by the SbF_6^- anion, which is engaged in a long secondary Au–F contact of 2.931(3) Å. Conversion of **1**-Cl into [**1**][SbF_6] induces a shortening of the Sb–Cl bond from 2.4829(13) Å in **1**-Cl to 2.4106(11) Å in [**1**][SbF_6]. This contraction reflects the increased Lewis acidity of the cationic antimony–gold complex. It also results in a lengthening of the Au–Sb bond from 2.8527(6) Å in **1**-Cl to 2.9318(5) Å in [**1**][SbF_6], which suggests a weakening of the Au–Sb interaction.

To better understand the nature of these changes, both **1**-Cl and $[\mathbf{1}]^+$ have been studied computationally using DFT methods (Gaussian program,[14] functional BP86;[15] mixed basis set Sb/Au cc-pVTZ-pp;[16] P/Cl 6-31g(d′), C/H 6-31g). The structure optimizations reproduce the trend observed experimentally, with **1**-Cl displaying a computed Au–Sb bond shorter (2.911 Å) than that of $[\mathbf{1}]^+$ (2.955 Å). Analyses of these structures using the natural bond orbital method (NBO) suggest that the Au–Sb interactions are weak and are best described as donor–acceptor interactions (Figure 2). As

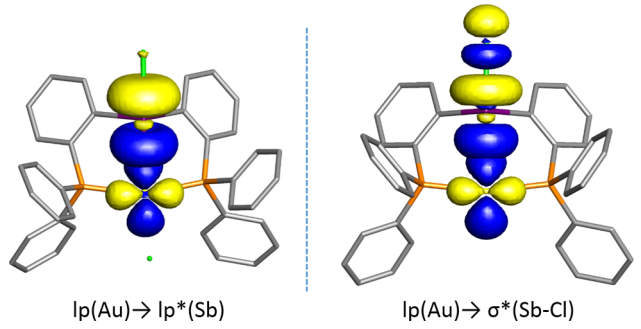

Figure 2. NBO plots of the major Sb–Au bonding interactions in **1**-Cl (left) and [**1**][SbF_6] (right) (isodensity value 0.05, the lp* orbital is a vacant Sb orbital of p character). Hydrogen atoms are omitted.

observed for other chlorostibine–gold complexes investigated by us,[5] the NBO analysis shows that **1**-Cl possesses a Au→Sb rather than a Sb→Au interaction. In turn, we conclude that the accepting properties of the chlorostibine moiety dominate its ligative characteristics, as observed for related chlorobismuthine complexes.[17] This interaction, which has lp(Au)→lp*(Sb) character, is associated with a deletion energy (or stabilization energy) E_{del} of 70.79 kcal/mol. The donicity of the gold center toward antimony is notably decreased in $[\mathbf{1}]^+$, which possesses a lp(Au)→σ*(Sb–Cl) interaction associated with a deletion energy E_{del} of only 28.29 kcal/mol. This decrease directly results from the removal of the gold-bound chloride anion positioned trans from the antimony atom. The removal of this ligand leads to a decreased electron density on the gold atom, which becomes a weaker donor toward antimony. Such effects have been previously discussed by Bourissou, who showed that conversion of the gold boratrane $[(o\text{-}(i\mathrm{Pr}_2\mathrm{P})\mathrm{C}_6\mathrm{H}_4)_3\mathrm{B}]\mathrm{AuCl}$ into its cationic counterpart $[((o\text{-}(i\mathrm{Pr}_2\mathrm{P})\mathrm{C}_6\mathrm{H}_4)_3\mathrm{B})\mathrm{Au}]^+$ is accompanied by a weakening of the Au→B interaction present in these complexes.[18]

The electronic structure of $[\mathbf{1}]^+$ is reminiscent of that displayed by cations of type $[\mathbf{D}]^+$ (Chart 3).[9] These cations, which are derived from the corresponding gold chloride complex **D**-Cl,[11d] have been reported as competent catalysts for reactions that necessitate alkyne activation. Because the chlorostibine moiety of $[\mathbf{1}]^+$ mimics the σ-acceptor properties of boron,[5] we decided to determine whether $[\mathbf{1}]^+$ could also be used for the activation of alkynes. To test this idea, we chose to study the hydroamination of alkynes, not only because of the synthetic importance of this reaction but also because of its

DOI: 10.1021/jacs.5b07998
J. Am. Chem. Soc. 2015, 137, 13425–13432

Chart 3. Side by Side Comparison Showing $[1]^+$ and a Recently Reported Boron Complex of Type $[D]^+$ [9,13]

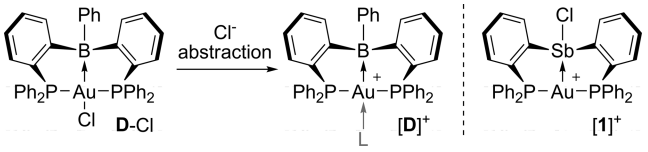

simplicity. A test reaction involving *p*-toluidine and phenylacetylene was carried out in $CDCl_3$ under ambient conditions, with a catalyst loading of 3.5 mol % (Scheme 2). Catalysts

Scheme 2. Model Hydroamination Reaction Used To Evaluate $[1][SbF_6]$

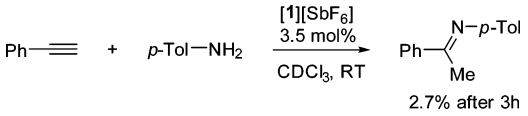

$[1][SbF_6]$ displayed a non-negligible but very low activity, with only 2.7% conversion into the Markovnikov imine product after 3 h. When the same reaction was repeated with $[(Ph_3P)_2Au]$-SbF_6 as a catalyst, no measurable conversion was observed. These results suggest that the chlorostibine moiety of $[1]^+$ plays an activating role, albeit a very weak one. This prompted us to question whether oxidation of the antimony atom could be used to strengthen the Au→Sb interaction, leading to a more acidic and thus more catalytically active gold center.

Gold–Trihalostiborane Complexes. With oxidation of the antimony center as a goal, complex **1** was allowed to react with $PhICl_2$ in CH_2Cl_2 (Scheme 3). This reaction afforded the

Scheme 3. Synthesis of 2-Cl, 3-Cl, and $[3][SbF_6]$ [13]

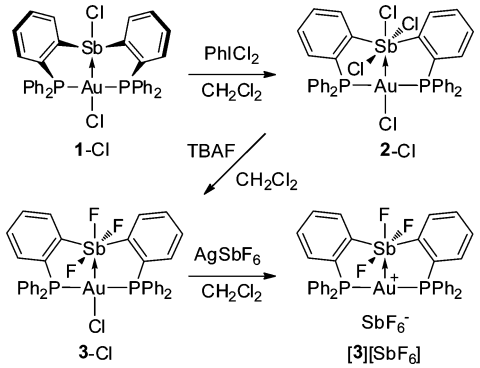

trichlorostiborane complex **2**-Cl as a pale yellow precipitate. The ^{31}P NMR spectrum of **2**-Cl shows a signal at 72.0 ppm, which is significantly downfield from that of complex **1**-Cl. Crystals of **2**-Cl were grown from CH_2Cl_2. Inspection of the structure confirms oxidation of the antimony center and formation of a trichlorostiborane unit that directly engages the gold atom in a Au→Sb interaction of 2.6985(14) Å (Figure 3). The Au–Sb bond is notably shorter than that in **1**-Cl (2.8527(6) Å), indicating that oxidation of the antimony center increases its Lewis acidity, leading to a stronger Au→Sb dative interaction. The gold atom displays a square-planar geometry which, as indicated by the Cl–Au–Sb angle (177.88(5)° in **2**-Cl vs 153.90(3)° in **1**-Cl), is much less distorted than in **1**-Cl. This square-planar geometry points to the trivalent character of the gold atom, providing further

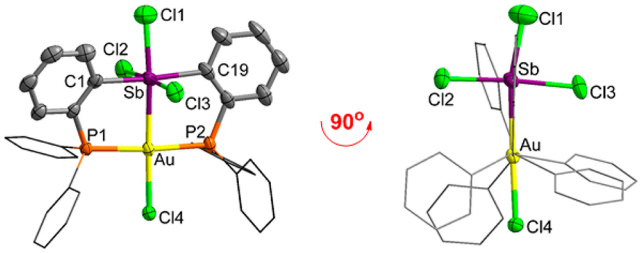

Figure 3. Solid-state structure of **2**-Cl. Thermal ellipsoids are drawn at the 50% probability level. Phenyl groups are drawn in wireframe. Hydrogen atoms are omitted for clarity. Relevant metrical parameters can be found in the text or in the Supporting Information.

support for the increased Au→Sb dative interaction upon oxidation of the antimony center. Finally, the antimony center adopts an octahedral geometry which shows little distortion, as indicated by the values of the Cl1–Sb–Au (167.95(11)°), Cl2–Sb–Cl3 (175.75(10)°), and C1–Sb–C19 angles (169.6(4)°). Complex **2**-Cl is poorly soluble in most organic solvents, including CH_2Cl_2 and $CHCl_3$, which complicated an exploration of its chemical reactivity. Confronted with this difficulty, we decided to explore the generation of a more soluble analogue. Gratifyingly, we observed that **2**-Cl could be easily converted into the more soluble trifluoride complex **3**-Cl by reaction with TBAF or TASF in CH_2Cl_2 (Scheme 3). The ^{31}P NMR resonance of **3**-Cl at 83.5 ppm is split into a doublet, indicating coupling to the axial antimony-bound fluorine atom ($J_{P-F_{ax}}$ = 16 Hz). The ^{19}F NMR spectrum shows two signals (Figure 4). The two equatorial fluorine atom give rise to a

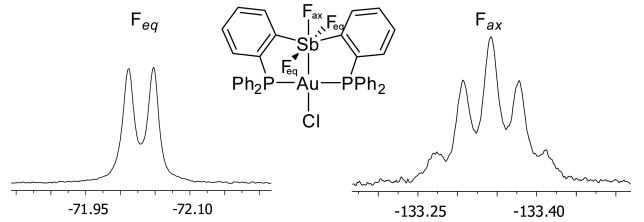

Figure 4. Resonances observed in the ^{19}F NMR spectrum of **3**-Cl measured in $CDCl_3$.

doublet at −72 ppm with $J_{F_{ax}-F_{eq}}$ = 17 Hz. The axial fluorine resonance appears as a pseudoquintet at −133 ppm because of the near-degeneracy of $J_{P-F_{ax}}$ (16 Hz) and $J_{F_{ax}-F_{eq}}$ (17 Hz). The absence of coupling between the phosphorus and equatorial fluorine nuclei is certainly noteworthy and may be rationalized by invoking the Karplus rule and the orthogonality of the F–Sb–F and P–Au–P vector. Crystals of **3**-Cl were readily obtained through Et_2O diffusion into a CH_2Cl_2 solution. The structure of **3**-Cl is very similar to that of **2**-Cl. The Sb–Au bond of 2.7069(7) Å in **3**-Cl is almost identical with that in **2**-Cl (2.6985(14) Å), suggesting little change in the Au→Sb interaction. As in **2**-Cl, (i) the gold atom of **3**-Cl adopts a square-planar geometry with a Cl–Au–Sb angle close to linearity (176.37(7)°) and (ii) the antimony atom, now at the center of a trifluorostiborane unit, retains an octahedral geometry (F1–Sb1–Au1 = 178.3(2)°, F2–Sb1–F3 = 179.2(3)°, and C1–Sb1–C19 = 173.7(3)°).

With the intent of accessing a well-defined alkyne activation catalyst, complex **3**-Cl was treated with $AgSbF_6$ in CH_2Cl_2, which resulted in the clean formation of the corresponding

DOI: 10.1021/jacs.5b07998
J. Am. Chem. Soc. 2015, 137, 13425–13432

cationic complex $[3]^+$ as a hexafluoroantimonate salt (Scheme 3). A similar reaction could not be cleanly carried out with **2**-Cl, which gave an intractable product mixture when treated with $AgSbF_6$. The salt $[3][SbF_6]$ has been characterized by ^{31}P NMR spectroscopy, which shows a resonance at 66.3 ppm. The ^{19}F NMR spectrum displays two new resonances corresponding to the axial (−147.1 ppm) and equatorial fluorine ligands (−55.1 ppm). In addition to chemical shift changes, these resonances are all singlets, indicating that the F−F and P−F scalar coupling has become too small to observe. The weakening of the Sb−Au bond upon conversion of **3**-Cl into $[3][SbF_6]$ (vide infra) may be responsible for the disappearance of the P−F scalar coupling. The disappearance of the F−F coupling is more difficult to rationalize but is nevertheless firmly established on the basis of the spectra. Crystals of $[3][SbF_6]$ could be obtained through pentane diffusion into a CH_2Cl_2 solution of the complex under moisture-free conditions. The main distinguishing feature in the structure of $[3][SbF_6]$ is a Au−Sb bond length of 2.8196(4) Å, which is significantly elongated in comparison to that in **3**-Cl (2.7069(7) Å) (Figure 5). As argued in the case of $[1][SbF_6]$, the removal

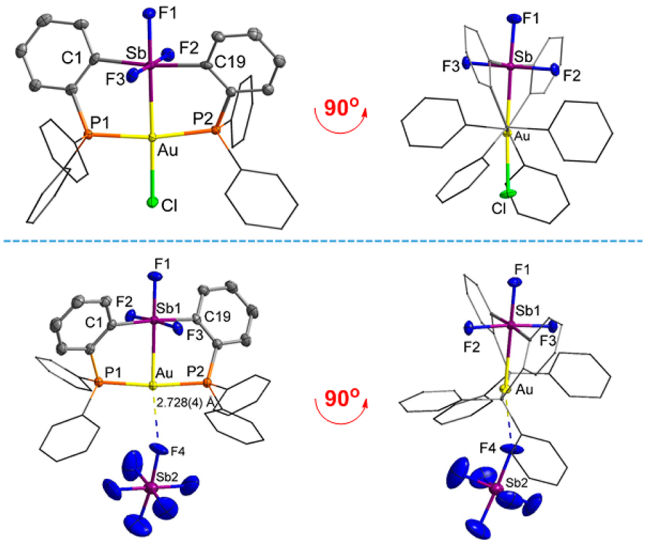

Figure 5. Solid-state structures of **3**-Cl (top) and $[3][SbF_6]$ (bottom). Thermal ellipsoids are drawn at the 50% probability level. Phenyl groups are drawn in wireframe. Hydrogen atoms and solvent molecules are omitted for clarity. Relevant metrical parameters can be found in the text or in the Supporting Information.

of the chloride anion from the gold center decreases the metallobasicity of the latter, leading to a weaker Au→Sb interaction.[18] This weaker Au→Sb dative bond also affects the length of the Sb−F bonds, which are notably shorter in $[3][SbF_6]$ ($Sb-F_{ax}$ = 1.942(7) Å in **3**-Cl vs 1.897(4) Å in $[3][SbF_6]$ and $Sb-F_{eq}$ = 1.961(6) Å in **3**-Cl vs 1.942(2) Å in $[3][SbF_6]$). The P(1)−Au−Sb, P(2)−Au−Sb, and P1−Au−P2 angles of 86.689(18), 86.689(18), and 173.38(4)°, respectively, suggest that the gold coordination geometry is best described as T-shaped. The structure of $[3][SbF_6]$ can also be compared with that of $[1][SbF_6]$. A comparison of the Au−Sb distance (2.9318(5) Å in $[1][SbF_6]$ vs 2.8196(4) Å in $[3][SbF_6]$) illustrates the higher acidity of the oxidized antimony center and the comparatively stronger Au→Sb dative interaction. Finally, the vacant site trans from the antimony is flanked by the SbF_6^- counteranion with which it forms an Au- - -F contact of 2.728(4) Å. The presence of this contact, which is shorter than that observed in $[1][SbF_6]$ (2.931(3) Å), attests to the greater Lewis acidity of the gold atom. In turn, these comparisons show that oxidation of the antimony center in $[3][SbF_6]$ translates into a stronger Au→Sb dative interaction and a harder gold atom.

Lewis Acidic Behavior and Electronic Structures of the Gold−Trihalostiborane Complexes. The increased hardness of the gold atom in $[3]^+$ is reminiscent of the mercury stibonium complex $[E]^+$, in which the Lewis acidity of the d^{10} ion is enhanced by juxtaposition with a strongly Lewis acidic pentavalent antimony moiety.[19] Complex $[E]^+$ forms adducts with both neutral and anionic donors (D), which coordinate to the mercury center in a direction perpendicular to the two primary ligands. The Lewis acidity enhancement observed for $[3]^+$ has the same origin: namely, the presence of an adjoining and highly acidic pentavalent antimony center. In support of this analogy, we observe formation of the water adduct $[3\text{-}OH_2][SbF_6]$, which was isolated as a byproduct in small quantities due to the presence of adventitious water

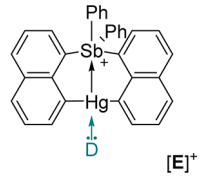

Scheme 4. Formation of $[3\text{-}OH_2][SbF_6]$[13]

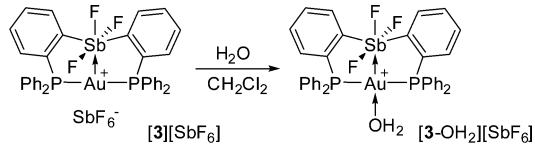

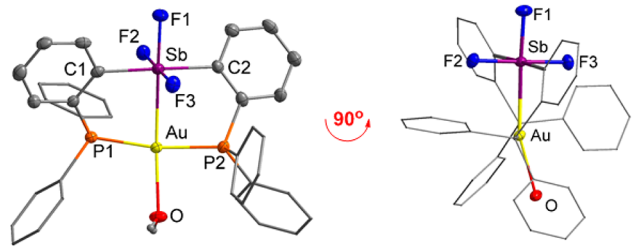

Figure 6. Solid-state structure of $[3\text{-}OH_2][SbF_6]$. Thermal ellipsoids are drawn at the 50% probability level. Phenyl groups are drawn in wireframe. Hydrogen atoms and solvent molecules are omitted for clarity. Relevant metrical parameters can be found in the text or in the Supporting Information.

(Scheme 4). X-ray analysis of this adduct (Figure 6) shows that the water ligand is coordinated to the gold center via a bond of length 2.383(3) Å. The Au−Sb bond of 2.7775(6) Å is intermediate between that of **3**-Cl (2.7069(7) Å) and $[3][SbF_6]$ (2.837(4) Å). Accordingly, the Sb−F bonds in the water adduct $[3\text{-}OH_2][SbF_6]$ ($Sb-F_{ax}$ = 1.914(3) Å and $Sb-F_{eq}$ = 1.947(3) Å) also fall between those in **3**-Cl and $[3][SbF_6]$ (*vide supra*). These structural features can be assigned to the donor strength of the water ligand, which is weaker than that of the chloride anion in **3**-Cl and yet stronger than that of the weakly coordinating SbF_6^- anion in $[3][SbF_6]$. The ability of

DOI: 10.1021/jacs.5b07998
J. Am. Chem. Soc. 2015, 137, 13425−13432

the gold center of $[3]^+$ to coordinate water bears a parallel with some recently described triorganogold(III) complexes, which engage water among other hard donors.[20] A further measure of the Lewis acidity of $[3]^+$ is provided by a simple Gutmann–Beckett measurement using $Ph_3P{=}O$ (δ 27.3, CH_2Cl_2) as a Lewis base. When the base is mixed 1/1 with a $[Au(PPh_3)_2]^+$ salt in CH_2Cl_2, no shift of the $Ph_3P{=}O$ ^{31}P NMR resonance is observed, indicating that coordination does not occur. When the same experiment is repeated with $[1][SbF_6]$ and $[3][SbF_6]$, the resonance shifts downfield to 30.6 and 32.9 ppm, respectively. These changes speak to the increased acidity of the gold atom imparted by the presence of a chlorostibine unit in $[1]^+$ and an oxidized trifluorostiborane unit in $[3]^+$.

The ligand push/antimony pull effects observed in these complexes can also be analyzed computationally. The structures of 3-Cl, $[3\text{-}OH_2][SbF_6]$, and $[3][SbF_6]$ have been optimized computationally at the same level of theory as that used for 1-Cl and $[1]^+$ (basis set for F 6-31+g(d′)) (Figure 7). The

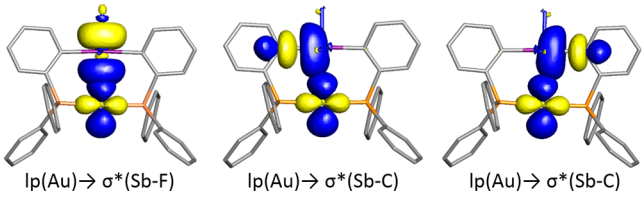

Figure 7. NBO plots of the major Sb–Au bonding interactions $[3]^+$ (isodensity value 0.05). Hydrogen atoms are omitted. The same donor–acceptor interactions are also observed for 3-Cl and $[3\text{-}OH_2]^+$.

lengthening of the Sb–Au bond observed experimentally on going from 3-Cl to $[3\text{-}OH_2]^+$ and $[3]^+$ is nicely reproduced computationally with distances of 2.76(6), 2.82(4), and 2.87(1) Å for these three compounds, respectively. The NBO analyses support the dative nature of the Au–Sb interaction (Figure 7). In addition to lp(Au)→σ*(Sb–F) interactions, each complex also features lp(Au)→σ*(Sb–C) donor–acceptor interactions that make an important contribution to the stability of the complexes. This is confirmed by deletion calculations, which afford E_{del} = 148.52, 91.18, and 59.18 kcal/mol for 3-Cl, $[3\text{-}OH_2]^+$, and $[3]^+$, respectively. These energies correlate with the donor strength of the ligand bound to gold and provide a further illustration of the ligand push/antimony pull effect at play in these complexes. Accordingly, the natural population analysis (NPA) charges calculated for the antimony atom of $[3]^+$ (2.312), $[3\text{-}OH_2]^+$ (2.274), and 3-Cl (2.139) decrease as the trans influence of the gold-bound ligand increases. The gold NPA charge also increases ($[3]^+$ (0.276), $[3\text{-}OH_2]^+$ (0.379), and 3-Cl (0.484)), suggesting a greater extent of Au→Sb electron transfer. Finally, a comparison of the Au→Sb stabilization energies in $[1]^+$ (28.29 kcal/mol) and $[3]^+$ (59.18 kcal/mol) illustrates the increased σ-accepting properties of the trifluorostiborane, which behaves as a Z-type ligand.

The increasing transfer of electron density from gold to antimony observed on going from $[3]^+$ to $[3\text{-}OH_2]^+$ and 3-Cl can also be depicted on the basis of the resonance structures shown in Figure 8. Structures of type **a** correspond to Au(I)–Sb(V) species with the gold atom in the monovalent state. Resonance structures of type **b**, which account for the donation of an electron pair from gold to antimony, correspond to Au(II)–Sb(IV) species. Remembering that valence and formal oxidation states are different concepts,[21] the gold atom in structures of type **b** is in the trivalent state. While both

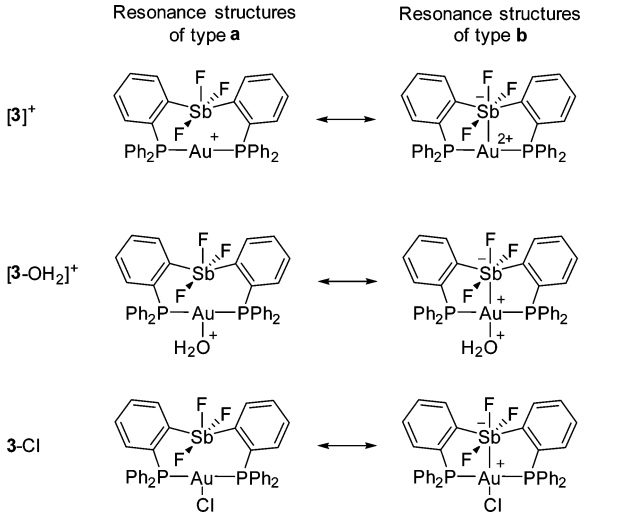

Figure 8. Resonance structures for $[3]^+$ to $[3\text{-}OH_2]^+$ and 3-Cl.[13]

resonance structures contribute to the electronic structures of all three complexes, the structural and computational results described above show that the importance of structure **b** increases on going from $[3]^+$ to $[3\text{-}OH_2]^+$ and 3-Cl. This smooth transition illustrates the dynamic and adaptive nature of the Au–Sb interaction, which increases in strength when the gold atom accepts a donor ligand.

Catalytic Properties of the Cationic Gold–Trifluorostiborane Salt [3][SbF$_6$]. With $[3][SbF_6]$ in hand, we became eager to test whether the stronger Au→Sb interaction would indeed correlate with a higher catalytic activity in reactions involving alkynes. While the reaction of *p*-toluidine and phenylacetylene was very poorly catalyzed by $[1][SbF_6]$, we found $[3][SbF_6]$ to be a very competent catalyst for this reaction, with an essentially complete conversion after 40 min at room temperature in $CDCl_3$, with a catalyst loading of 3.5 mol % (Table 1, entry 1). Carrying out the reaction under strictly anhydrous conditions or in air gives identical results, suggesting that adventitious water does not inhibit the activity of the catalysts. In fact, when $[3][SbF_6]$ is treated with *p*-toluidine (4 equiv) in CH_2Cl_2, the ^{31}P NMR resonance of the complex shifts from 63.6 to 76.5 ppm while the ^{19}F NMR resonances shift from −52.3 and −148.8 ppm to −63.0 and −140.1 ppm. These changes suggest coordination of *p*-toluidine to the gold center of $[3]^+$ in solution. No notable changes are observed when $[3][SbF_6]$ is treated with phenylacetylene in CH_2Cl_2. The coordination of amines to gold hydroamination catalysts is not unprecedented. It is usually assumed that these adducts dissociate prior to activation of the alkyne.[22] Since many late-transition-metal hydroamination catalysts,[7,23] including those with gold,[8] often necessitate an inert atmosphere, high temperature, and relatively long reaction time, the fact that $[3][SbF_6]$ catalyzes the reactions under mild conditions and in air is noteworthy. We have also carried out this reaction on a larger scale (6.5 mmol), with a lower catalyst loading (0.5 mol %). Full conversion was also observed but necessitated a longer reaction time of 6 h. We have studied the scope of this reaction with bulky, electron-rich, and/or electron-poor amines. As shown in Table 1, hydroamination of phenylacetylene with the bulky 2,6-diisopropylaniline gave 93% of the desired products in 70 min under ambient conditions (entry 2).[8h,23b] The reaction proceeded more slowly with the electron-poor pentafluoroani-

DOI: 10.1021/jacs.5b07998
J. Am. Chem. Soc. 2015, 137, 13425–13432

Table 1. Results Obtained in the Hydroamination of Terminal Alkynes with Aromatic Amines with [3]SbF_6 as a Catalyst

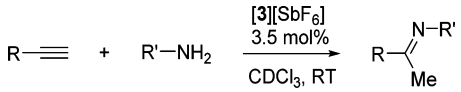

Entry	R—	H_2N–R'	N–R'	t	Conv. (Yield)[a]
1			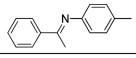	40 min	98 % (92%)
2			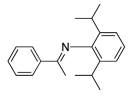	70 min	93% (83%)
3			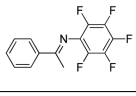	48 h	68%
4			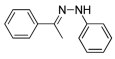	30 min	86% (72%)
5			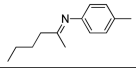	60 min	61%

[a]The conversion (conv.) was measured by ^{1}H NMR spectroscopy using an internal standard. The yield given in parentheses corresponds to the isolated yield.

line, affording a 68% yield after 48 h (entry 3). The low yield of this reaction is caused by partial hydrolysis of the imine product and formation of acetophenone. The reaction also proceeded quickly with phenylhydrazine (entry 4) but failed with alkylamines such as cyclohexylamine, which on the basis of NMR spectroscopy lead to formation of multiple species, suggesting catalyst decomposition. We also examined the hydroamination reactions of the less activated terminal aliphatic alkyne. 1-Hexyne reacted with *p*-toluidine to produce the desired imine within 60 min (entry 5).

CONCLUSIONS

In this paper, we have shown that the σ-accepting properties of chlorostibine ligands can be greatly enhanced by oxidative conversion into the corresponding trihalostiboranes. This increase leads to a strengthening of the Au→Sb interaction. As a result of this strengthening, the gold center of $[\mathbf{3}]^+$ acquires a trivalent character, making it a harder Lewis acid, as confirmed by the isolation of a water adduct. More importantly, the changes induced by oxidation of the antimony center also affect the reactivity of the gold center, making $[\mathbf{3}]^+$ a competent catalyst for the hydroamination of alkynes.

EXPERIMENTAL SECTION

General Considerations. [(tht)AuCl] (tht = tetrahydrothiophene)[24] and $PhICl_2$[25] were prepared according to the reported procedures. Solvents were dried by passing through an alumina column (*n*-pentane and CH_2Cl_2) or by reflux under N_2 over Na/K (Et_2O and THF). All other solvents were used as received. Commercially available chemicals were purchased and used as provided (commercial sources: Aldrich for $SbCl_3$ and Bu_4NF; Strem Chemicals for $AgSbF_6$). Ambient-temperature NMR spectra were recorded on a Varian Unity Inova 500 FT NMR spectrometer (499.42 MHz for ^{1}H, 125.58 MHz for ^{13}C, 469.89 MHz for ^{19}F, 202.16 MHz for ^{31}P). Chemical shifts δ are given in ppm and are referenced against residual solvent signals (^{1}H, ^{13}C) or external $BF_3{\cdot}Et_2O$ (^{19}F) and H_3PO_4 (^{31}P).

Synthesis of 1-Cl. A CH_2Cl_2 solution (8 mL) of (tht)AuCl (250 mg, 0.78 mmol) was slowly added to a CH_2Cl_2 solution (10 mL) of L^{Cl} (530 mg, 0.78 mmol) at ambient temperature. After the mixture was stirred for 12 h, the solvent was removed under vacuum, affording an oily residue. This residue was treated with Et_2O (10 mL), leading to the precipitation of **1**-Cl as a yellow solid. Compound **1**-Cl was dried under vacuum and obtained in a 93% yield (660 mg). Crystals of **1**-Cl·$2CH_2Cl_2$ suitable for X-ray diffraction were obtained by slow diffusion of Et_2O into a concentrated CH_2Cl_2 solution of **1**-Cl at low temperature (2−8 °C). ^{1}H NMR (499.42 MHz; $CDCl_3$): δ 7.01 (m, 2 H, *o*-P(Sb)C_6H_4), 7.35 (t, 2 H, *o*-P(Sb)C_6H_4, $^3J_{H-H}$ = 7.49 Hz), 7.45−7.54 (m, 16 H), 7.64 (t, 2 H, *o*-P(Sb)C_6H_4, $^3J_{H-H}$ = 7.49 Hz), 7.86 (m, 4 H), 8.59 (d, 2 H, *o*-P(Sb)C_6H_4, $^3J_{H-H}$ = 7.49 Hz). ^{13}C{^{1}H} NMR (125.58 MHz; $CDCl_3$): δ 128.5 (q, J_{C-P} = 28.9 Hz), 129.3 (t, J_{C-P} = 4.0 Hz), 129.4 (t of d, −C_6H_5, CH, J_{C-P} = 42.7 Hz, J = 5.9 Hz), 131.9 (d, −C_6H_5, CH, J_{C-P} = 4.9 Hz), 132.7 (s), 133.5 (t, J_{C-P} = 2.8 Hz), 134.2 (t of d, −C_6H_5, CH, J_{C-P} = 24.6 Hz, J = 7.2 Hz), 135.3 (t, J_{C-P} = 8.5 Hz), 137.7 (t, J_{C-P} = 29.1 Hz), 149.3 (t, J_{C-P} = 17.7 Hz). ^{31}P{^{1}H} NMR (202.16 MHz; $CDCl_3$): δ 38.4 (s). Mp: 186 °C dec. Anal. Calcd for **1**-Cl·$2CH_2Cl_2$ ($C_{38}H_{32}Cl_6P_2AuSb$): C, 42.18; H, 2.98. Found: C, 43.25; H, 3.15. These elemental analysis results may suggest partial loss of the interstitial CH_2Cl_2. Anal. Calcd for **1**-Cl·$1.5CH_2Cl_2$ ($C_{37.5}H_{31}Cl_5P_2AuSb$): C, 43.33; H, 3.01. For additional information on the purity of this compound, please see the NMR spectra provided in the Supporting Information.

Synthesis of [1][SbF_6]. A CH_2Cl_2 (1 mL) solution of $AgSbF_6$ (15.5 mg, 45 μmol) was slowly added to a CH_2Cl_2 solution (2 mL) of complex **1**-Cl (41 mg, 45 μmol). The resulting cloudy solution was stirred for 15 min, filtered, and analyzed by ^{31}P NMR spectroscopy, which confirmed full conversion of **1**-Cl into [**1**][SbF_6]. The salt [**1**][SbF_6] was purified by evaporation of the solvent and washing with two portions of Et_2O (2 mL). The salt [**1**][SbF_6] was obtained in 56% yield (38 mg) as a pale yellow powder. Light yellow plates of [**1**][SbF_6]·CH_2Cl_2 were obtained by slow diffusion of Et_2O into a concentrated CH_2Cl_2 solution of [**1**][SbF_6] at room temperature. ^{1}H NMR (499.42 MHz; $CDCl_3$): δ 7.15 (q, 2 H, *o*-P(Sb)C_6H_4, $^3J_{H-H}$ = 6.49 Hz), 7.51 (q, 6 H, $^3J_{H-H}$ = 7.49 Hz), 7.60 (t, 4 H, $^3J_{H-H}$ = 7.49 Hz), 7.64−7.66 (m, 12 H), 7.72 (t, 2 H, $^3J_{H-H}$ = 7.99 Hz), 8.48 (d, 2 H, *o*-P(Sb)C_6H_4, $^3J_{H-H}$ = 7.49 Hz). ^{13}C{^{1}H} NMR (125.58 MHz; $CDCl_3$): δ 125.0 (t, J_{C-P} = 30.9 Hz), 125.8 (t, J_{C-P} = 30.1 Hz), 130.3 (t of d, −C_6H_5, CH, J_{C-P} = 37.7 Hz, J = 6.0 Hz), 131.1 (t, J_{C-P} = 4.5 Hz), 133.3 (s, −C_6H_5, CH), 133.6 (s), 133.9 (t, J_{C-P} = 4.2 Hz), 134.1 (t of d, −C_6H_5, CH, J_{C-P} = 27.9 Hz, J = 7.4 Hz), 135.3 (t, J_{C-P} = 7.8 Hz), 148.8 (t, J_{C-P} = 16.1 Hz). ^{31}P{^{1}H} NMR (202.16 MHz; $CDCl_3$): δ 50.3 (s). Mp: 255 °C dec. Anal. Calcd for [**1**][SbF_6]·CH_2Cl_2 ($C_{37}H_{30}Cl_3F_6P_2AuSb_2$): C, 37.11; H, 2.53. Found: C, 37.58; H, 2.53. For additional information on the purity of this compound, please see the NMR spectra provided in the Supporting Information.

Synthesis of 2-Cl. A CH_2Cl_2 solution (5 mL) of $PhICl_2$ (151 mg, 0.55 mmol) was slowly added to a CH_2Cl_2 solution (8 mL) of **1**-Cl (387 mg, 0.42 mmol) at ambient temperature, resulting in the slow precipitation of the product. After 2 h, the resulting mixture was evacuated to dryness and the resulting pale yellow residue was washed with ether. This procedure afforded **2**-Cl in 94% yield (390 mg). Complex **2**-Cl is only slightly soluble in $CHCl_3$ and CH_2Cl_2. Single crystals of **2**-Cl were obtained by slow evaporation of the CH_2Cl_2 solution. ^{1}H NMR (499.42 MHz; $CDCl_3$): δ 7.41 (t of d, 2 H, *o*-P(Sb)C_6H_4, $^3J_{H-H}$ = 6.49 Hz, $^3J_{H-P}$ = 4.00 Hz), 7.47 (t 10 H, $^3J_{H-H}$ = 7.49 Hz), 7.54 (t, 4 H, *o*-P(Sb)C_6H_4, $^3J_{H-H}$ = 7.49 Hz), 7.65 (q 8 H, $^3J_{H-H}$ = 6.99 Hz), 7.74 (t, 2 H, $^3J_{H-H}$ = 8.49 Hz), 9.44 (d, 2 H, *o*-P(Sb)C_6H_4, $^3J_{H-H}$ = 7.99 Hz). ^{31}P{^{1}H} NMR (202.16 MHz; $CDCl_3$): δ 79.2 (s). The poor solubility of this product did not allow for a satisfactory ^{13}C NMR spectrum to be collected. Mp: 220 °C dec. Anal. Calcd for **2**-Cl ($C_{36}H_{28}Cl_4P_2AuSb$): C, 43.98; H, 2.87. Found: C, 43.30; H, 2.81. For additional information on the purity of this compound, please see the NMR spectra provided in the Supporting Information.

Synthesis of 3-Cl. TBAF·$3H_2O$ (530 mg, 1.68 mmol) dissolved in CH_2Cl_2 (6 mL) was added was added within 1 min to a CH_2Cl_2 (10 mL) suspension of **2**-Cl (460 mg, 0.47 mmol). The yellowish

DOI: 10.1021/jacs.5b07998
J. Am. Chem. Soc. 2015, 137, 13425−13432

suspension of **2**-Cl became immediately clear and colorless. After the mixture was stirred for 2 h, the solvent was removed under vacuum. The withe residue was washed with three portions of methanol (4 mL) and dried under vacuum, affording **3**-Cl in 91% yield (397 mg). Colorless crystals of **3**-Cl·CH_2Cl_2 were easily obtained by slow diffusion of ether into a CH_2Cl_2 solution. ^{1}H NMR (499.42 MHz; $CDCl_3$): δ 7.40−7.48 (m, 12H), 7.53 (t, 4 H, *o*-P(Sb)C_6H_4, $^3J_{H-H}$ = 7.00 Hz), 7.60 (q 8 H, $^3J_{H-H}$ = 7.00 Hz), 7.70 (q, 2 H, $^3J_{H-H}$ = 8.00 Hz), 8.74 (d, 2 H, *o*-P(Sb)C_6H_4, $^3J_{H-H}$ = 8.00 Hz). $^{13}C\{^1H\}$ NMR (125.58 MHz; $CDCl_3$): δ 121.8 (broad, weak, t, J_{C-P} = 29.5 Hz), 127.0 (t, J_{C-P} = 31.0 Hz), 127.4 (t, J_{C-P} = 31.3 Hz), 129.0 (t of d, −C_6H_5, CH, J_{C-P} = 7.8 Hz, J_{C-F} = 5.9 Hz) 130.9 (t of d, J_{C-P} = 11.8 Hz, J_{C-F} = 3.1 Hz), 132.3 (d, −C_6H_5, CH, J_{C-P} = 3.6 Hz), 133.3 (d, J_{C-P} = 17.1 Hz), 133.8 (broad), 134.0 (t of d, −C_6H_5, CH, J_{C-P} = 9.4 Hz, J_{C-F} = 6.4 Hz), 134.9 (m). $^{31}P\{^1H\}$ NMR (202.16 MHz; $CDCl_3$): δ = 83.5 (d, $J_{P-F_{ax}}$ = 16.2 Hz). $^{19}F\{^1H\}$ NMR (469.89 MHz; $CDCl_3$): δ −72.0 (d, $2F_{eq}$, $J_{F_{eq}-F_{ax}}$ = 17.0 Hz), −133.3 (pseudoquintet, $1F_a$, $J_{F_{ax}-F_{eq}}$ = 17.0 Hz, $J_{F_{ax}-P}$ = 16.2 Hz). Mp: 238 °C dec. Anal. Calcd for **3**-Cl ($C_{36}H_{28}ClF_3P_2AuSb$): C, 46.31; H, 3.02. Found: C, 46.01; H, 3.22. For additional information on the purity of this compound, please see the NMR spectra provided in the Supporting Information.

Synthesis of [3][SbF_6]. A CH_2Cl_2 (2 mL) solution of $AgSbF_6$ (73.6 mg, 0.21 mmol) was slowly added to a CH_2Cl_2 solution (3 mL) of complex **3**-Cl (200 mg, 0.21 mmol). The resulting cloudy solution was stirred for 1 h, filtered, and analyzed by ^{31}P NMR spectroscopy, which confirmed full conversion of **3**-Cl into [**3**][SbF_6]. The salt [**3**][SbF_6] was isolated by evaporation of the solvent and washing with two portions of Et_2O (2 mL). The salt [**3**][SbF_6] was obtained in 75% yield (184 mg) as a colorless powder. Crystals of [**3**][SbF_6] were obtained by slow diffusion of pentane into a concentrated CH_2Cl_2 solution at room temperature under an inert atmosphere using a glovebox. ^{1}H NMR (499.42 MHz; $CDCl_3$): δ 7.37 (q, 2 H, $^3J_{H-H}$ = 5.99 Hz), 7.54−7.66 (m, 22H), 7.79 (t, 2 H, $^3J_{H-H}$ = 7.99 Hz), 8.42 (d, 2 H, *o*-P(Sb)C_6H_4, $^3J_{H-H}$ = 7.99 Hz) $^{13}C\{^1H\}$ NMR (125.58 MHz; $CDCl_3$): δ 124.7 (t, J_{C-P} = 30.8 Hz), 130.1 (t, −C_6H_5, CH, J_{C-P} = 6.03 Hz), 132.2 (t, J = 4.02 Hz), 133.5 (s, −C_6H_5, CH), 134.1 (t, −C_6H_5, CH, J_{C-P} = 7.16 Hz), 134.1 (s), 135.7 (s), quaternary carbon nuclei not detected. $^{31}P\{^1H\}$ NMR (202.16 MHz; $CDCl_3$): δ 66.3 (s). $^{19}F\{^1H\}$ NMR (469.89 MHz; $CDCl_3$): δ −55.1 (s, $2F_{eq}$), −147.0 (s, $1F_a$), −122.3 (broad, SbF_6). Mp: 205 °C dec. Anal. Calcd for [**3**][SbF_6] ($C_{36}H_{28}F_9P_2AuSb$): C, 38.13; H, 2.49. Found: C, 37.86; H, 2.44. For additional information on the purity of this compound, please see the NMR spectra provided in the Supporting Information.

General Procedure for Catalytic Hydroamination Reactions. Catalytic reactions were carried out in air. In a typical reaction, the alkyne (∼0.5 mmol) was mixed with the amine (∼0.55 mmol) in $CDCl_3$ (2 mL). After addition of the catalyst (3.5 mol % loading), conversion was estimated using ^{1}H NMR spectroscopy with 1,4-di-*tert*-butylbenzene.

Computational Details. Density functional theory (DFT) structural optimizations were carried with the Gaussian 09 suite of programs with effective core potentials on all heavy atoms (functional BP86; mixed basis set Sb/Au cc-pVTZ-PP, P/Cl 6-31g(d), C/O/H 6-31g, F 6-31+g(d′)). The optimized structures were subjected to a NBO analysis.[26] The resulting NBOs were visualized and plotted with the Jimp 2 program.[27]

Crystallographic Measurements. The crystallographic measurements were performed at 110(2) K using a Bruker APEX-−II CCD area detector diffractometer (Mo Kα radiation, λ = 0.71069 Å). In each case, a specimen of suitable size and quality was selected and mounted onto a nylon loop. The structures were solved by direct methods, which successfully located most of the non-hydrogen atoms. Semiempirical absorption corrections were applied. Subsequent refinement on F^2 using the SHELXTL/PC package (version 6.1) allowed location of the remaining non-hydrogen atoms.

■ ASSOCIATED CONTENT

Supporting Information

The Supporting Information is available free of charge on the ACS Publications website at DOI: 10.1021/jacs.5b07998.

Additional experimental and computational details (PDF)
Optimized stuructures (XYZ)
Crystallographic data (CIF)

■ AUTHOR INFORMATION

Corresponding Author

*E-mail for F.P.G.: francois@tamu.edu.

Notes

The authors declare no competing financial interest.

■ ACKNOWLEDGMENTS

This work was supported by the National Science Foundation (CHE-1300371), the Welch Foundation (A-1423), and Texas A&M University (Arthur E. Martell Chair of Chemistry).

■ REFERENCES

(1) (a) Levason, W.; McAuliffe, C. A. *Acc. Chem. Res.* **1978**, *11*, 363−368. (b) Champness, N. R.; Levason, W. *Coord. Chem. Rev.* **1994**, *133*, 115−217. (c) Silvestru, C.; Breunig, H. J.; Althaus, H. *Chem. Rev.* **1999**, *99*, 3277−3328. (d) Schulz, S. *Coord. Chem. Rev.* **2001**, *215*, 1−37. (e) Schulz, S. *Struct. Bonding (Berlin)* **2006**, *103*, 117−166. (f) Breunig, H. J.; Ghesner, I. *Adv. Organomet. Chem.* **2003**, *49*, 95−131. (g) Werner, H. *Angew. Chem., Int. Ed.* **2004**, *43*, 938−954. (h) Levason, W.; Reid, G. *Coord. Chem. Rev.* **2006**, *250*, 2565−2594. (i) Burt, J.; Levason, W.; Reid, G. *Coord. Chem. Rev.* **2014**, *260*, 65−115.

(2) (a) Benjamin, S. L.; Levason, W.; Reid, G.; Warr, R. P. *Organometallics* **2012**, *31*, 1025−1034. (b) Benjamin, S. L.; Levason, W.; Light, M. E.; Reid, G.; Rogers, S. M. *Organometallics* **2014**, *33*, 2693−2695.

(3) (a) Shriver, D. F. *Acc. Chem. Res.* **1970**, *3*, 231−238. (b) Dammann, C. B.; Hughey, J. L.; Jicha, D. C.; Meyer, T. J.; Rakita, P. E.; Weaver, T. R. *Inorg. Chem.* **1973**, *12*, 2206−2209. (c) Chan, D. M. T.; Marder, T. B. *Angew. Chem., Int. Ed. Engl.* **1988**, *27*, 442−443. (d) Parkin, G. *Organometallics* **2006**, *25*, 4744−4747. (e) Hill, A. F. *Organometallics* **2006**, *25*, 4741−4743. (f) Fontaine, F.-G.; Boudreau, J.; Thibault, M.-H. *Eur. J. Inorg. Chem.* **2008**, *2008*, 5439−5454. (g) Braunschweig, H.; Dewhurst, R. D.; Schneider, A. *Chem. Rev.* **2010**, *110*, 3924−3957. (h) Bouhadir, G.; Amgoune, A.; Bourissou, D. *Adv. Organomet. Chem.* **2010**, *58*, 1−107. (i) Amgoune, A.; Bourissou, D. *Chem. Commun.* **2011**, *47*, 859−871. (j) Braunschweig, H.; Dewhurst, R. D. *Dalton Trans.* **2011**, *40*, 549−558. (k) Bauer, J.; Braunschweig, H.; Dewhurst, R. D. *Chem. Rev.* **2012**, *112*, 4329−4346. (l) Owen, G. R. *Chem. Soc. Rev.* **2012**, *41*, 3535−3546. (m) Kameo, H.; Nakazawa, H. *Chem. - Asian J.* **2013**, *8*, 1720−1734. (n) Mingos, D. M. P. *J. Organomet. Chem.* **2014**, *751*, 153−173.

(4) (a) Wade, C. R.; Gabbaï, F. P. *Angew. Chem., Int. Ed.* **2011**, *50*, 7369−7372. (b) Ke, I.-S.; Jones, J. S.; Gabbaï, F. P. *Angew. Chem., Int. Ed.* **2014**, *53*, 2633−2637. (c) Wade, C. R.; Ke, I.-S.; Gabbaï, F. P. *Angew. Chem., Int. Ed.* **2012**, *51*, 478−481. (d) Jones, J. S.; Wade, C. R.; Gabbaï, F. P. *Angew. Chem., Int. Ed.* **2014**, *53*, 8876−8879.

(5) Ke, I.-S.; Gabbaï, F. P. *Inorg. Chem.* **2013**, *52*, 7145−7151.

(6) Anderson, J. S.; Rittle, J.; Peters, J. C. *Nature* **2013**, *501*, 84−87.

(7) (a) Huang, L.; Arndt, M.; Gooßen, K.; Heydt, H.; Gooßen, L. J. *Chem. Rev.* **2015**, *115*, 2596−2697. (b) Mizushima, E.; Chatani, N.; Kakiuchi, F. *J. Organomet. Chem.* **2006**, *691*, 5739−5745.

(8) (a) Hahn, C.; Cruz, L.; Villalobos, A.; Garza, L.; Adeosun, S. *Dalton Trans.* **2014**, *43*, 16300−16309. (b) Wang, Y.; Wang, Z.; Li, Y.; Wu, G.; Cao, Z.; Zhang, L. *Nat. Commun.* **2014**, *5*, 3470. (c) Anokhin, M. V.; Murashkina, A. V.; Averin, A. D.; Beletskaya, I. P. *Mendeleev Commun.* **2014**, *24*, 332−333. (d) Malhotra, D.; Mashuta, M. S.;

DOI: 10.1021/jacs.5b07998
J. Am. Chem. Soc. 2015, 137, 13425−13432

Hammond, G. B.; Xu, B. *Angew. Chem., Int. Ed.* **2014**, *53*, 4456−4459. (e) Gonell, S.; Poyatos, M.; Peris, E. *Angew. Chem., Int. Ed.* **2013**, *52*, 7009−7013. (f) Lavallo, V.; Wright, J. H.; Tham, F. S.; Quinlivan, S. *Angew. Chem., Int. Ed.* **2013**, *52*, 3172−3176. (g) Alvarado, E.; Badaj, A. C.; Larocque, T. G.; Lavoie, G. G. *Chem. - Eur. J.* **2012**, *18*, 12112−12121. (h) Dash, C.; Shaikh, M. M.; Butcher, R. J.; Ghosh, P. *Inorg. Chem.* **2010**, *49*, 4972−4983. (i) Leyva, A.; Corma, A. *Adv. Synth. Catal.* **2009**, *351*, 2876−2886. (j) Lavallo, V.; Frey, G. D.; Donnadieu, B.; Soleilhavoup, M.; Bertrand, G. *Angew. Chem., Int. Ed.* **2008**, *47*, 5224−5228. (k) Mizushima, E.; Hayashi, T.; Tanaka, M. *Org. Lett.* **2003**, *5*, 3349−3352.

(9) Inagaki, F.; Matsumoto, C.; Okada, Y.; Maruyama, N.; Mukai, C. *Angew. Chem., Int. Ed.* **2015**, *54*, 818−822.

(10) (a) Slone, C. S.; Mirkin, C. A.; Yap, G. P. A.; Guzei, I. A.; Rheingold, A. L. *J. Am. Chem. Soc.* **1997**, *119*, 10743−10753. (b) Wang, X.; Thevenon, A.; Brosmer, J. L.; Yu, I.; Khan, S. I.; Mehrkhodavandi, P.; Diaconescu, P. L. *J. Am. Chem. Soc.* **2014**, *136*, 11264−11267.

(11) (a) Devillard, M.; Nicolas, E.; Appelt, C.; Backs, J.; Mallet-Ladeira, S.; Bouhadir, G.; Slootweg, J. C.; Uhl, W.; Bourissou, D. *Chem. Commun.* **2014**, *50*, 14805−14808. (b) Fong, H.; Moret, M.-E.; Lee, Y.; Peters, J. C. *Organometallics* **2013**, *32*, 3053−3062. (c) Harman, W. H.; Peters, J. C. *J. Am. Chem. Soc.* **2012**, *134*, 5080−5082. (d) Sircoglou, M.; Bontemps, S.; Mercy, M.; Saffon, N.; Takahashi, M.; Bouhadir, G.; Maron, L.; Bourissou, D. *Angew. Chem., Int. Ed.* **2007**, *46*, 8583−8586.

(12) Yang, H.; Gabbaï, F. P. *J. Am. Chem. Soc.* **2014**, *136*, 10866−10869.

(13) In this paper, all cationic bis(phosphine)gold complexes are depicted with a positive charge on the gold atom, in line with the notion that these complexes contain a gold(I) cation ligated by two neutral phosphine ligands. These moieties could also be depicted as bis(phosphonium)aurates of the type $(R_3P^+)_2Au^-$ with a positive formal charge on each phosphorus atom and a negative charge on the gold atom.

(14) Frisch, M. J.; Trucks, G. W.; Schlegel, H. B.; Scuseria, G. E.; Robb, M. A.; Cheeseman, J. R.; Scalmani, G.; Barone, V.; Mennucci, B.; Petersson, G. A.; Nakatsuji, H.; Caricato, M.; Li, X.; Hratchian, H. P.; Izmaylov, A. F.; Bloino, J.; Zheng, G.; Sonnenberg, J. L.; Hada, M.; Ehara, M.; Toyota, K.; Fukuda, R.; Hasegawa, J.; Ishida, M.; Nakajima, T.; Honda, Y.; Kitao, O.; Nakai, H.; Vreven, T.; Montgomery, J. A., Jr.; Peralta, J. E.; Ogliaro, F.; Bearpark, M.; Heyd, J. J.; Brothers, E.; Kudin, K. N.; Staroverov, V. N.; Kobayashi, R.; Normand, J.; Raghavachari, K.; Rendell, A.; Burant, J. C.; Iyengar, S. S.; Tomasi, J.; Cossi, M.; Rega, N.; Millam, J. M.; Klene, M.; Knox, J. E.; Cross, J. B.; Bakken, V.; Adamo, C.; Jaramillo, J.; Gomperts, R.; Stratmann, R. E.; Yazyev, O.; Austin, A. J.; Cammi, R.; Pomelli, C.; Ochterski, J. W.; Martin, R. L.; Morokuma, K.; Zakrzewski, V. G.; Voth, G. A.; Salvador, P.; Dannenberg, J. J.; Dapprich, S.; Daniels, A. D.; Farkas, Ö.; Foresman, J. B.; Ortiz, J. V.; Cioslowski, J.; Fox, D. J. *Gaussian 09, Revision B.01*; Gaussian, Inc., Wallingford, CT, 2009.

(15) (a) Becke, A. D. *Phys. Rev. A: At., Mol., Opt. Phys.* **1988**, *38*, 3098−3100. (b) Perdew, J. P. *Phys. Rev. B: Condens. Matter Mater. Phys.* **1986**, *33*, 8822−8824.

(16) (a) Peterson, K. A.; Figgen, D.; Goll, E.; Stoll, H.; Dolg, M. *J. Chem. Phys.* **2003**, *119*, 11113−11123. (b) Figgen, D.; Rauhut, G.; Dolg, M.; Stoll, H. *Chem. Phys.* **2005**, *311*, 227−244.

(17) (a) Tschersich, C.; Limberg, C.; Roggan, S.; Herwig, C.; Ernsting, N.; Kovalenko, S.; Mebs, S. *Angew. Chem., Int. Ed.* **2012**, *51*, 4989−4992. (b) Lin, T.-P.; Ke, I.-S.; Gabbaï, F. P. *Angew. Chem., Int. Ed.* **2012**, *51*, 4985−4988.

(18) Sircoglou, M.; Bontemps, S.; Bouhadir, G.; Saffon, N.; Miqueu, K.; Gu, W.; Mercy, M.; Chen, C.-H.; Foxman, B. M.; Maron, L.; Ozerov, O. V.; Bourissou, D. *J. Am. Chem. Soc.* **2008**, *130*, 16729−16738.

(19) (a) Lin, T.-P.; Wade, C. R.; Pérez, L. M.; Gabbaï, F. P. *Angew. Chem., Int. Ed.* **2010**, *49*, 6357−6360. (b) Lin, T.-P.; Nelson, R. C.; Wu, T.; Miller, J. T.; Gabbaï, F. P. *Chem. Sci.* **2012**, *3*, 1128−1136.

(20) Wu, C.-Y.; Horibe, T.; Jacobsen, C. B.; Toste, F. D. *Nature* **2015**, *517*, 449−454.

(21) Parkin, G. *J. Chem. Educ.* **2006**, *83*, 791−799.

(22) Widenhoefer, R. A.; Han, X. *Eur. J. Org. Chem.* **2006**, *2006*, 4555−4563.

(23) (a) Alex, K.; Tillack, A.; Schwarz, N.; Beller, M. *ChemSusChem* **2008**, *1*, 333−338. (b) Chen, Q.; Lv, L.; Yu, M.; Shi, Y.; Li, Y.; Pang, G.; Cao, C. *RSC Adv.* **2013**, *3*, 18359−18366. (c) Hartung, C. G.; Tillack, A.; Trauthwein, H.; Beller, M. *J. Org. Chem.* **2001**, *66*, 6339−6343. (d) Klein, D. P.; Ellern, A.; Angelici, R. J. *Organometallics* **2004**, *23*, 5662−5670. (e) Tokunaga, M.; Eckert, M.; Wakatsuki, Y. *Angew. Chem., Int. Ed.* **1999**, *38*, 3222−3225.

(24) Uson, R.; Laguna, A.; Laguna, M. *Inorg. Synth.* **1989**, *26*, 85−91.

(25) Zhao, X.-F.; Zhang, C. *Synthesis* **2007**, *2007*, 551−557.

(26) Glendening, E. D.; Badenhoop, J. K.; Reed, A. E.; Carpenter, J. E.; Bohmann, J. A.; Morales, C. M.; Weinhold, F.; *NBO 5.9*; Theoretical Chemistry Institute, University of Wisconsin, Madison, WI, 2011.

(27) Manson, J.; Webster, C. E.; Pérez, L. M.; Hall, M. B.: http://www.chem.tamu.edu/jimp2/index.html.

DOI: 10.1021/jacs.5b07998
J. Am. Chem. Soc. 2015, 137, 13425−13432